Materials Science-Poland, 40(4), 2022, pp. 114-124
http://www.materialsscience.pwr.wroc.pl/
DOI: 10.2478/msp-2022-0048

sciendo

A new approach to flux deposition for brazing aluminium by low pressure cold spraying

Tomasz Wojdat[1,*], Marcin Winnicki[1], Jaroslaw Pabian[2]

[1]Department of Metal Forming, Welding and Metrology, Wroclaw University of Science and Technology, Wrocław, Poland
[2]Mahle Behr Corp., Ostrów Wielkopolski, Poland

This paper presents the results of study on the possibility of Nocolok flux deposition to aluminium substrates using the low-pressure cold gas spraying (LPCS) method. An innovative method of applying flux in the form of a powder without organic adhesive additives was proposed, allowing strict control of the deposited material. The influence of the flux powder feeding rate (PFR – 4.5 g/min, 6.3 g/min and 8.5 g/min) on the efficiency of the brazing process of AA3003 aluminium alloy plates was investigated. The results of energy dispersive spectrometry (EDS) analysis of the deposited flux coatings are presented for various process parameters. The wettability tested by spreading the B-AlSi12 filler metal on flux-covered aluminium substrates increased significantly with increasing PFR – the contact angle decreased from 21.0° to 4.6°. Microstructure analysis confirmed the high quality of the brazed joints, which were devoid of braze incompatibilities.

Keywords: *flux deposition, low-pressure cold spraying, aluminium alloy, brazing, flux powder, brazed joints, B-AlSi12 filler metal*

1. Introduction

Brazing aluminium with the use of fluxes, that is, auxiliary substances, is fast, simple and effective [1], and thus is very popular in the automotive and aviation industries [2]. A large field of application of flux brazing is the production of aluminium heat exchangers [3]. The process contains many parts, such as heater core, condenser, evaporator, transmission oil cooler, engine oil cooler, charge air cooler, fuel cooler and so on [4]. These components are usually made of EN AW-3003 and EN AW-3005 alloys containing manganese [5], which increases the mechanical properties and resistance to corrosion [6]. Additionally, the alloys show good formability, for example, by stamping and rolling, and can be applied at elevated temperatures [7]. The dominant technology in these industries is controlled atmosphere brazing (CAB) performed in continuous furnaces [8]. In the case of brazing of aluminium alloys, the most used shielding gas against air access is high-purity nitrogen [2–4]. However, it is not sufficient for high-quality brazing of Al alloys, and therefore non-corrosive flux should be used as an additional material [9].

The brazeability of aluminium alloys is influenced by their physicochemical properties, that is, high thermal expansion and thermal conductivity. However, a very high affinity of aluminium to oxygen results in the formation of chemically stable aluminium oxides with a high melting point of 2,037°C [10]. Al_2O_3 significantly decreases the wettability of the alloy by the filler metal. Therefore, immediately prior to CAB brazing, the surface of the aluminium alloy should be pre-cleaned from oxides and constantly protected during the process to avoid reoxidation [6]. For this purpose, braze fluxes are used [11]. One of the most applied non-corrosive fluxes in aluminium brazing is the inorganic fluoride salt $K_{1-3}AlF_{4-6}$, known as Nocolok [12].

The basic factor influencing the brazing efficiency and joint quality is the flux application method. There are several methods of flux application, and the most popular are the following: (i) spraying an aqueous flux suspension, (ii) spraying flux in the form of paint (called Paint-Flux), (iii) application of a flux paste and (iv) electrostatic ap-

* E-mail: tomasz.wojdat@pwr.edu.pl

© Wojdat et al. 2022. This is an open access article distributed under the Creative Commons Attribution-NonCommercial-NoDerivatives 4.0 License. (http://creativecommons.org/licenses/by-nc-nd/4.0/)

plication of flux with the use of a mixture of flux and air [4]. The final choice depends on the production volume, geometry of the covered elements, efficiency, economic considerations and so on [4]. However, it should be emphasised that each method has various drawbacks and limitations, while the most troublesome is the precise control of the flux mass per unit area and the presence of organic adhesive in Paint-Flux.

The improper flux mass occurs as a deficiency or excess of the flux. The former hinders the brazing process and deteriorates the joint quality, while the latter causes problems related to the efficient functioning of the exchanger under operating conditions. What is more, the new ecological restrictions limit the flux residue mass generated in the brazing process and are therefore strictly defined by the customer in the specification.

Flux residues on the external surfaces of the exchanger are troublesome, because they can decrease its efficiency by limiting the ability to remove heat but are not removed after the brazing process [13]. Considerably more problematic are flux residues trapped inside the exchanger due to the high reactivity to coolants and the formation of 'gelling' [5]. Consequently, clogging of one of the heat exchangers occurs, usually with the smallest pipe cross-section [5]. Therefore, the mass of flux residues for a cooler-type exchanger, depending on the geometry of the part, should be in the range of 0.4–2.5 g [14].

Another problem is the presence of various additions, for example, an organic adhesive in Paint-Flux, which ensured good adhesion of the deposited flux to the substrate. The Paint-Flux consists of flux, 20–45 wt.%, organic adhesive, 5–10 wt.%, and demineralised water, balance [13]. The post-deposited flux undergoes drying to combine the flux with the surface. However, the high efficiency makes the technology applicable in manufacturing complex heat exchangers. The organic adhesive agent should evaporate completely during the preheating stage and prior to the brazing process. Nevertheless, sheets stacked on top of each other in complex exchangers significantly reduce the evaporation of organic adhesives. As a result, the residues trapped between the sheets carbonise at the brazing temperature (577–605°C) [14], forming various types of brazing incompatibilities, for example, porosity, voids and often under-brazing [14]. The incompatibilities significantly reduce the active surface of the joint.

Excluding braze incompatibilities is impossible with current flux application technology, which causes many production defects. Most of the produced exchangers do not show any leaks, but unfortunately rarely withstand the pressure tests, which causes loss of braze cohesion [14]. According to the SIST EN 378-2 standard, the test pressure should be 1.5 times higher than the maximum working pressure [15].

The main goal of this study was to develop and validate the flux application technology, which would enable the elimination or significant reduction of the faulty products that accompany the currently used method. Therefore, we proposed a kinetic process, low-pressure cold spraying (LPCS), which, compared with the currently used methods of applying fluxes, has several advantages, and the most important are: (i) precise control of the flux amount per unit area, (ii) application of pure powder materials instead of water suspensions with the addition of organic adhesives, (iii) no shape limitations, (iv) no surface preparation needed, (v) unsettled powder recovery and (vi) high efficiency and economy of the process. In the LPCS powder particles are accelerated by working gas and gain supersonic velocity in the de Laval nozzle. Additional preheating of the gas increases the velocity and kinetic energy of the particles as well [16–18]. It should be emphasised that the process temperature is maintained below the chemical activation point of the powder to avoid oxidation, melting, and so on, and depends on the sprayed material [19–21]. Eventually, solid-state particles impacting the substrate interlock mechanically and form a coating. LPCS is commonly used to spray metal or metal–ceramic composite coatings. However, the latest research showed that it can be used in the deposition of ceramic powders [22–24]. Therefore, in this paper, we tested flux deposition by LPCS as well as the brazeability of prepared samples.

Table 1. LPCS process parameters during flux deposition

Powder feed rate, g/min	Traverse speed, mm/s	Gas preheating temperature, °C	Gas pressure, MPa	Stand-off, mm	Number of spray passes
4.5 6.3 8.5	20	200	05	10	1

2. Materials and methods

Nocolok flux (Solvay, Belgium) powder with irregular shape and an average particle size of 2–6 μm was deposited by LPCS. The chemical composition of the flux was as follows: 28–31 wt.% K, 16–18 wt.% Al, 49–53 wt.% F, max. 2.5 wt.% LOH [11]. The flux was applied using DYMET 413 (Obninsk Center for Powder Spraying, Obninsk, Russia) LPCS device. A standard circular de Laval nozzle with a throat diameter to outlet diameter ratio of 1:2 formed a spray jet. Compressed air was used as the propellant gas. The spraying gun with an internal electrical heater was attached to a manipulator (BZT Maschinenbau GmbH, Leopoldshöhe, Germany), moving with a traverse speed of 20 mm/s along parallel lines with 2-mm intervals. The process parameters are presented in Table 1. The combination of a low preheating gas temperature of 200°C and a high gas pressure of 0.9 MPa was selected to avoid activation of the flux in the stream and to eliminate the clogging of the nozzle by the powder, respectively. The thickness deposited flux was regulated by the powder feed rate. The parameters were selected based on the authors' previous research.

As-received aluminium alloy 3003 (AA3003) without any additional surface preparation or cleaning served as the substrate. Two sample sizes with dimensions of 1.6 mm × 50 mm × 50 mm and 2 mm × 25 mm × 80 mm were selected for the wettability test and the brazeability test, respectively. The melting point of the alloy is in the range of 640–655°C [25]. Therefore, the eutectic alloy B-AlSi12 (EN AW-4047) with 12 wt.% of Si and the smallest melting range of 577–582°C was used as a filler metal in the brazing process [26]. It should be noted that the filler was compatible with the flux activity temperature being in the range of 567–572°C [27].

A preliminary analysis of the surface topography and cross-section of flux coatings was performed using Keyence VHX6000 digital microscope (DM) and Hitachi TM3000 scanning electron microscope (SEM) equipped with an energy dispersive spectrometry (EDS) detector. Additionally, Keyence VHX6000 DM was used for roughness measurements. Five single profiles with a length of 3 mm were analysed according to the EN ISO 4287 standard and the average Ra value was determined.

The spreadability and wettability assessment was carried out in the flow test of 0.2 g of B-AlSi12 filler metal on AA3003 substrates with predeposited flux. The samples were placed on a ceramic stand and placed in the furnace (Nabertherm LT9/12, Lilienthal, Germany) heated to 600°C for 120 s and then cooled along with the furnace. The heating and cooling were performed under a nitrogen atmosphere. Later, the samples were cleaned of flux residues by rinsing them under running water. The small flux residues were easy to remove, which is favourable considering the application of LPCS in the process of spraying flux on elements of aluminium heat exchangers. Mean values were obtained from five measurements for each PFR sample. The surface area was chosen as a criterion for assessing spreadability. The larger the area of the sample surface occupied by the braze, the higher the spreadability. In the experiment, the only variable that influenced the result of the braze spreading was the amount of flux deposited on the substrate in the LPCS process.

To determine wettability, samples with a solidified drop of filler metal were cut in the middle and the contact angle was measured. According to

the criteria of brazeability assessment [28–30], the smaller the value of the contact angle, the better the wettability of the material. The wetting angles and surface areas of the spread filler metal were measured using DM.

The brazing process was carried out in accordance with the brazing procedures for aluminium heat exchangers under industrial conditions. Aluminium samples were positioned in a lap joint with an overlap length and width of 10 ± 1 mm and 25 mm, respectively. The brazing gap was set using steel spacer wires with a diameter of 0.2 mm. The joints were brazed in an electrical furnace (Nabertherm LT9/12, Lilienthal, Germany) under a nitrogen shielding atmosphere (Nitrogen 5.0, Linde gas). The wire of B-AlSi12 filler metal with diameter of 1.6 mm was cut into 25 mm pieces and placed at one end of the overlap. The braze filled the solder gap over the entire surface of the tab in molten form due to capillary action.

The brazing temperature and time were set to 600 ± 2°C and 120 s, respectively. The heating speed was 24°C/min, to ensure the so-called short brazing cycle time according to the temperature profiles of heat exchangers used in the automotive industry [4]. However, the brazing time was halved, due to the much smaller sample sizes (lower heat capacity) compared with the dimensions of the actual heat exchanger. Later, the microstructure of the samples was analysed using DM and SEM.

Microsections for metallographic observations were prepared by pouring samples in epoxy resin, which, after hardening, were subjected to grinding. The microsections were ground on water-abrasive papers with a gradation of 400–2500 – the rotational speed during grinding was 250 rpm. In the last stage, the samples were polished using a diamond suspension with grain sizes of 3 μm and 1 μm, respectively.

3. Results and discussion

3.1. Preliminary quality evaluation of the sprayed flux layers

In industry, the flux is applied to the surface of the heat exchanger elements by the wet or electrostatic (dry) method [31]. As shown in [32], the use of the dry method has a positive effect on improving the quality of the brazed joints. The use of the wet method increases the risk of contamination of the flux suspension with, for example, dust, metal particles and so on, and requires additional drying after the application process. Milani [33] showed that proper drying influences the mechanical properties of brazed joints and reduces the number of defective heat exchangers in production. Thus, the application of flux with the dry method shows several advantages over the wet method, and the proposed LPCS technology is a new method.

The LPCS process was used to spray the Nocolok flux on AA3003 substrate with three different powder feed rates (PFR): 4.5 g/min (PFR 1); 6.3 g/min (PFR 2); and 8.5 g/min (PFR 3). The calculated flux load on the surface as a coating given by grams of flux per square meter was following: 78.3 g/m^2 (PFR 1), 223.1 g/m^2 (PFR 2), and 708.3 g/m^2 (PFR 3).

The roughness of the coatings surface after the LPCS process is presented in Table 2. The most uniform and smooth coating with Ra equal to 16.1 μm showed the sample PFR 1. The Ra roughness of the samples increased with increasing powder feed rate and reached 35.7 μm for coating PFR 3. Figure 1 shows an exemplary measured roughness profile for the PFR 2 sample. It is well known that all thermal spray processes produce coatings with a developed surface area. However, the final coating roughness depends on the grain size of the powder and process parameters as well [X].

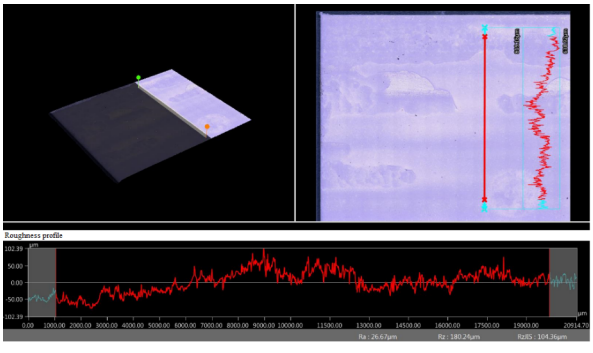


Fig. 1. An exemplary roughness profile for the PFR 2 sample (DM). DM, digital microscope

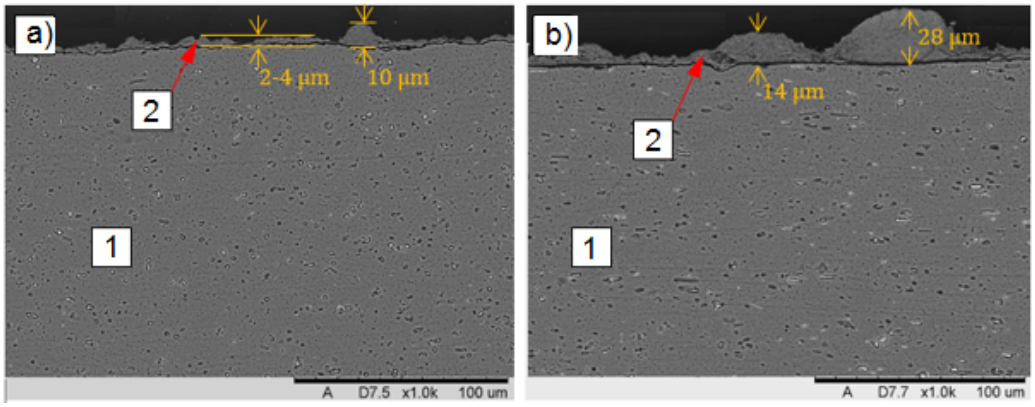


Fig. 2. Micrographs (SEM, BSE) of flux coatings: (A) PFR 1 and (B) PFR 2. 1 – substrate (AA3003), 2 – flux (Nocolok) coating. SEM, scanning electron microscope

Table 2. Results of roughness and thickness measurements

Parameter	Samples		
	PFR 1	PFR 2	PFR 3
Mean roughness *Ra* (µm)	16.1	24.3	35.7
Mean thickness *t* (µm)	5.3	16.2	83.5

Cross-sections of the coatings showed and confirmed the results of topographic analysis. The thickness of the coatings is uneven and strongly depends on the mass of the deposited flux (Table 2). The thinnest was the PFR 1 coating with thickness ranging from 2 µm to 10 µm (Figure 2A), while the PFR 2 coating showed the highest variation of the local thickness from 5 µm to 30 µm (Figure 2B).

The microstructure of the sample PFR 3 (Figure 3) revealed the most uniform and evenly distributed flux coating with a thickness in the range of 70–90 µm. In the LPCS process, the working gas decompresses in the divergent part of the de Laval nozzle, which is accompanied by a decreasing temperature [34–36]. However, the temperature can be regulated and increased by increased mass of powder particles, which are introduced at the beginning of the divergent part of the nozzle, where the gas temperature is the highest [37]. Therefore, increasing the amount of powder fed to the nozzle increased the temperature of the spraying jet. As a result, the thickness of the PFR 2 and PFR 3 coatings were enhanced. What is more, the irregular flux powder formed agglomerates that were responsible for the generation of surface roughness (see peaks in Figure 2). However, the value of the powder feed rate in sample PFR 3 seemed to be optimal as it significantly increased the thickness and stabilised the roughness. The applied flux layer was dense and continuous.

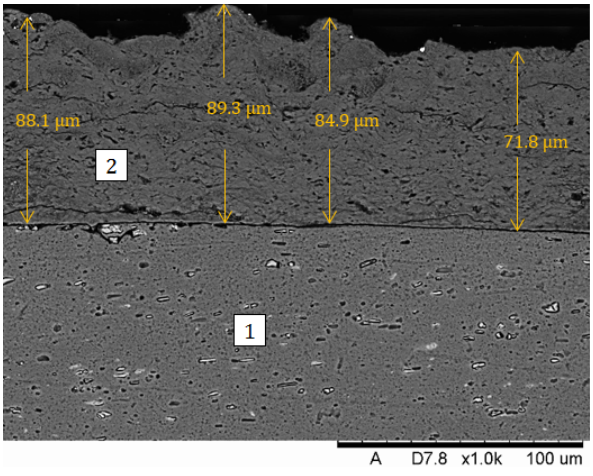
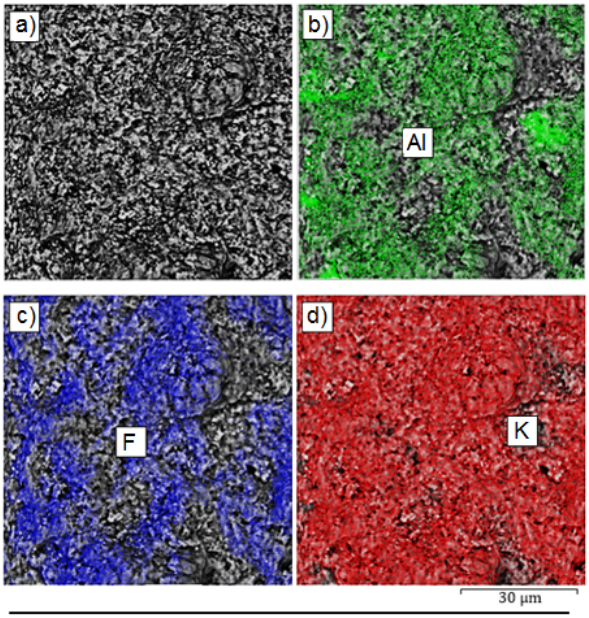


Fig. 3. Micrograph (SEM, BSE) of the PFR 3 coating. 1 – substrate (AA3003), 2 – flux (Nocolok) coating. SEM, scanning electron microscope

The chemical composition of the deposited flux coatings for individual PFR samples and determined based on the EDS surface analysis is given in Figure 4. The coatings consisted of the main components of the Nocolok flux, that is, K, F and Al. The distribution of individual elements was uniform over the entire surface of the samples (Fig-

ure 4). EDS analysis showed the highest fraction of fluorine (52.9 wt.%) and potassium (28.3 wt.%) in the PFR 3 sample; however, the elements were within the concentration range given in the manufacturer's specification [11]. In the case of samples PFR 1 and 2, the detector indicated the increased Al content, above 20 wt.%, due to locally uncoated substrate or too thin flux coating.



Powder Feed Rate, g/min	Chemical composition, wt%			
	K	Al	F	O
4.5	24.9	26.3	47.1	1.7
6.3	26.8	22.3	49.3	2.2
8.5	28.3	16.5	52.9	2.5

Fig. 4. (A) EDS analysis of the PFR 3 coating's surface and (B) elements distribution of aluminium, (C) fluorine and (D) potassium. Table – chemical composition of the coating depended on powder feed rate determined based on the surface EDS analysis. EDS, energy dispersive spectrometry

Regardless of the PFR, the applied flux layer adheres well to the substrate. It should be stressed that in electrostatic deposition, the achievement of good adhesion of the coating is largely dependent on the particle size distribution, but it is always quite low [32].

3.2. Brazing process – spreadability and wettability tests

The spreadability and wettability evaluation of the filler metal was performed by a flow test. The mean values of the spread areas are presented in Figure 5. The spreadability of the B-AlSi12 braze on the aluminium substrate with LPCS deposited flux was very good. The two smallest values of the spread areas in the range from 87 mm^2 to 141 mm^2 and 188 mm^2 to 205 mm^2 showed samples PFR 1 and PFR 2, respectively. The highest spreadability, in the range of 305–357 mm^2, was obtained for sample PFR 3. Furthermore, the smallest standard deviation of the PFR 3 sample confirmed its highest stability. An exemplary photo of the samples after the spreadability test with the measured surface area of the solidified filler metal is presented next to the bar in Figure 5.

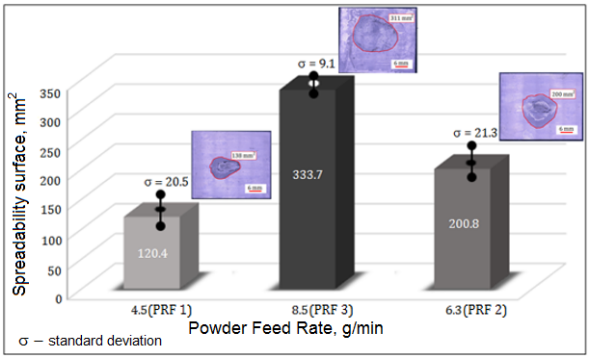


Fig. 5. Results of the B-AlSi12 filler metal spreadability on AA3003 substrates

The results of contact angle measurements for all coatings with exemplary images of the samples are presented in Figure 6. A very good wettability was obtained according to the spreading criteria [30], that is, a contact angle of less than 30°. Similarly, as for the spreadability results, the best wettability showed sample PFR 3 having the thickest flux coating. The measured contact angles were in the range of 3.9°–5.0°, while the mean value was equal to 4.6°. Sample PFR 2 with contact angles in the range of 10.5°–12.6° and an average value of 11.5° was comparable to PFR 1. The highest values of contact angle in the range of 20.2°–23.1° and the mean value of 21° were obtained for sample

PFR 1, which was coated with the lowest amount of flux. Flow tests strongly depend on the substrate activation by the flux [38]. Applying an appropriate amount of flux ensures complete elimination of the oxides present on the metal surface. When the flux coating is insufficient, that is, discontinuous or too thin, the oxide residues significantly limit the spread of molten filler metal [39]. As a result, the material is characterised by weak spreadability and wettability due to very small spread area and the solidified filler metal in the form of riser head [40].

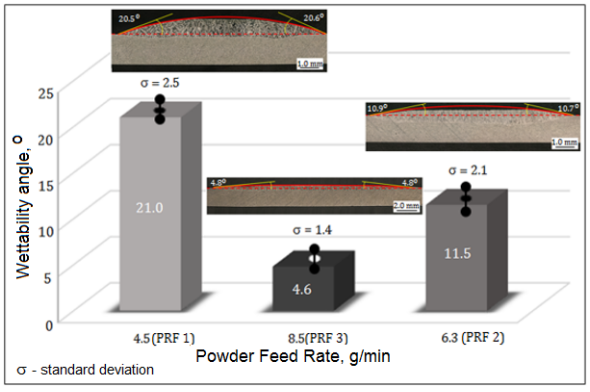


Fig. 6. Results of the B-AlSi12 filler metal wettability test on AA3003 substrates

3.3. Brazing of Aluminium Joints

The quality assessment was made by joining together AA3003 samples with pre-deposited flux. For the lowest powder feed rate (4.5 g/min, PFR 1), the amount of flux deposited in the spraying process was insufficient to make a brazed joint. The shortage of flux made it impossible to fill the gap by filler metal due to capillary action along the entire length of the overlap. On the opposite side to which the filler metal was applied, there is a 3-mm long fragment of the joint unfilled by the braze (Figure 7A). Moreover, the lack of free flow of the braze through the entire joint gap intensified the erosion phenomenon. As a result, the base material was dissolved due to the longer contact time with the liquid braze, which is known as 'guttering' [41]. What is more, an increase in the width of the braze gap occurred. A similar mechanism was also observed and described by Mirski and Pabian [4]. For the other two samples, that is, PFR 2 and PFR 3, the brazed joints were obtained. However, the quality depended strongly on the amount of the deposited flux (Figures 7B and 7C). Therefore, in the PFR 2 sample some pores were found at the joint (Figure 8B). Whereas, sample PFR 3 showed the highest quality, with no visible braze incompatibility (Figure 8C). Moreover, the free flow of the braze through both PFR 2 and PFR 3 joint gaps did not intensify the erosion phenomenon and the gap width remained constant along the entire length of the joint. To prevent the pores formation some authors suggest application expensive and time-taking vacuum brazing [42].

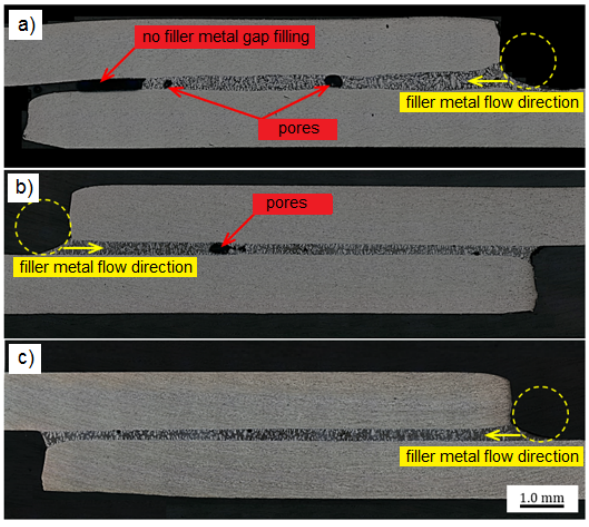


Fig. 7. Cross-section (DM) of brazed joints for various samples: (A) PFR 1, (B) PFR 2 and (C) PFR 3. DM, digital microscope

The microstructure of individual brazed joints was similar and consisted of the dendrites of the α-Al solution (1) crystallising from the diffusion zone towards the centre of the braze and the $\alpha + Si$ eutectic (2) localised in the inter-dendritic spaces (see Figure 8). However, differences between the size of the dendrites can be found. In the PFR 1 sample, where the erosion phenomenon was observed, the dendrites of the α-solution have a significantly higher volume (Figure 8A) compared with the other two joints, PFR 2 and PFR 3 (Figures 8B and 8C). It resulted from the dissolving of the aluminium substrate and addition of Al to the

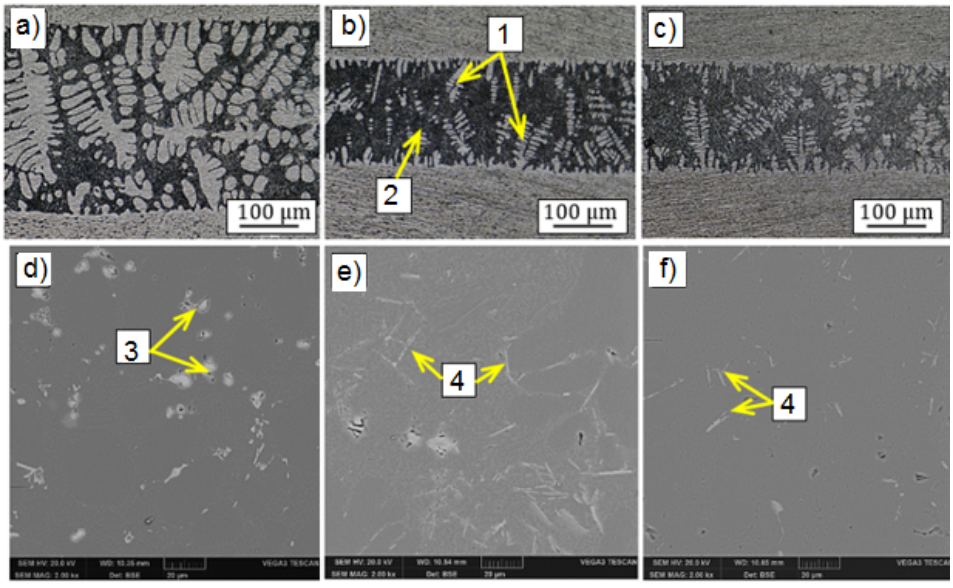


Fig. 8. Microstructure (SEM, BSE) of brazed joints (A) PFR 1, (B) PFR 2, (C) PFR 3 and phase precipitates of Si in the microstructure of (A) PFR1, (B) PFR 2 and (C) PFR 3 samples. 1 – solid solution dendrites α-Al, 2 – eutectic (α + *Si*), 3 – irregularly shaped intermetallic phase and 4 – coniferous Si phase precipitates. SEM, scanning electron microscope

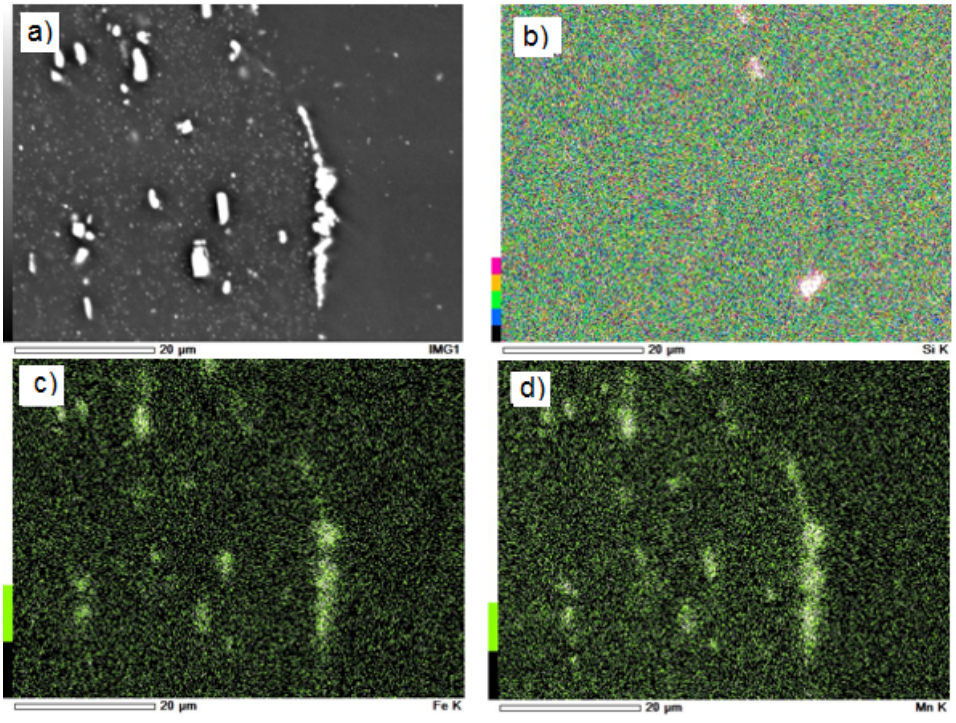
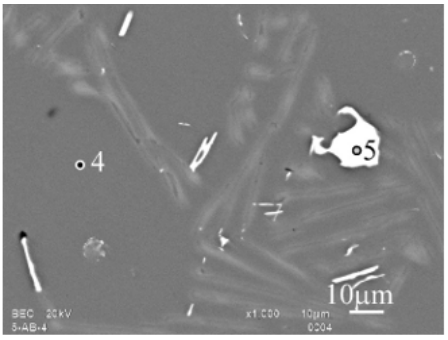


Fig. 9. EDS of the PFR 1 sample presenting the (A) analysed region and (B) distribution of the elements: Si, (C) Fe, and (D) Mn (mag. 2,000×, 20 keV). EDS, elemental mapping



	Al		Si		Mn		Fe	
Point	% mas.	% at.	% mas.	% at.	% mas.	% at.	% mas.	% at.
4	99.7		0.3		-		-	
5	61.1	72.1	9.9	11.3	11.5	6.7	17.5	9.9

Fig. 10. SEM micrograph (BSE) of the PFR 1 sample with EDS analysis (magnification 2,000×, 20 keV). EDS, energy dispersive spectrometry; SEM, scanning electron microscope

braze [4, 10]. What is more, the width of the braze increased double, while the thickness of the base material was reduced.

The brazing process initiated diffusion that influenced the microstructure of the samples. Fundamental alloy additives of the 3XXX aluminium alloy series are Mn, Fe and Si. The heavy elements, that is, Fe and Mn, are concentrated mainly in the base materials (Figure 9). The microstructure of the PFR 2 and PFR 3 joints showed mainly coniferous precipitates (4) (Figures 8E and 8F), which are typical for the Al-Si eutectic structure [27]. However, in the microstructure of the PFR 1 joint, additional irregularly shaped precipitates (3) were found (Figure 8D). It arose from the intense dissolution ('guttering') of the aluminium substrate. Elemental composition data in the sample area confirmed the presence of a complex Al-Fe-Mn-Si precipitates (Figure 10), which is probably the intermetallic phase $Al_{15}(Fe,Mn)_3Si_2$ [43].

4. Conclusions

This research showed that the LPCS method can be used successfully to apply flux to the surface of components intended for the brazing process. However, the optimisation of LPCS spray parameters prior to the brazing process are needed to improve the brazed joint quality.

As shown in the tests, an insufficient amount of flux, obtained for the lowest powder feed rate of 4.5 g/min, caused deterioration in the wettability of the brazed substrate, and consequently, hindered the correct execution of the brazed joint. In addition, the limited wettability intensified the dissolution of the brazed substrate, changing the geometry of the joint. Increasing the powder feed rate improved the quality of the brazed joint. The braze with excellent wettability and spreadability of 4.6° and 333.7 mm^2, respectively, and free from braze incompatibility, provided a powder feed rate of 8.5 g/min. However, simultaneously, it enlarges the production costs due to greater flux consumption and lengthens the time to remove the flux residue leftovers after the brazing process. Therefore, a medium powder feed rate of 6.3 g/min, which ensured a good wettability of 11.5° and allowed the acquisition of brazed joints that meet the quality requirements, appears to be the optimal value in the LPCS process.

Funding

This research received no external funding.

Conflict of interest

The authors declare no conflict of interest.

References

[1] Fabian R. *Vacuum technology: practical heat treating and brazing*. ASM International; Ohio, 1993.

[2] Singh M, Ohji T, Asthana R. *Green and sustainable manufacturing of advanced material*. Oxford (UK): Elsevier; 2015.

[3] Shah RK. Advances in automotive heat exchanger technology. *SAE Int*. 2003;112: 631–41.

[4] Mirski Z, Pabian J. Modern trends in production of brazed heat exchangers for automotive industry. *Weld Technol Rev*. 2017;89(8): 5–12.

[5] Mirski Z, Pabian J, Wojdat T, Hejna J. Significance of the brazing gap in the brazing of aluminium heat exchangers for automotive industry. *Weld Technol Rev*. 2020;92(4): 7–14.

[6] Woods R. CAB brazing metallurgy. 12th annual international invitational aluminum brazing seminar. Michigan (MI), USA: AFC Holcroft, NOVI; 2007.

[7] Kuczmaszewski J, Zalewski K. *Machining of aluminum and magnesium alloys*. Lublin, Poland: Lublin University of Technology; 2015.

[8] Orman L, Swidersky HW, Lauzon D. Brazing of aluminium alloys with higher magnesium content using non-corrosive fluxes. *Alum Brazing*. 2014;52: 24–9.

[9] Zhao H, Woods R. 10 – Controlled atmosphere brazing of aluminum. In: Dušan P Sekulić (ed.) *Woodhead publishing series in welding and other joining technologies*. *Adv Brazing*. Woodhead Publishing; Sawston (UK), 2013. p. 280–23.

[10] Mirski Z, Granat K, Misiek A. Brazing of aluminum heat exchangers in the automotive industry. *Spajanie materiałów konstrukcyjnych*. 2015;28(2): 32–4.

[11] Hu J, Zhang Q. Investigation of pseudo-ternary system AlF3–KF–KCl. *Thermochim Acta*. 2003;404(1–2): 3–7.

[12] Markovits T, Takács J, Lovas A, Belt J. Laser brazing of aluminium. *J Mater Process Technol*. 2003;143–144: 651–5.

[13] Pabian J. Analysis of erosion phenomena in brazing of aluminum heat exchangers. Scientific seminar. Wrocław, Poland: Wroclaw University of Technology; 2018.

[14] Orman L. *Quality tests of brazed plate heat exchangers using paint flux technology*. Internal Report for Valeo. Valeo, Skawina, Poland; 2017.

[15] European Committee for Electrotechnical Standardization (CENELEC). *Refrigerating systems and heat pumps - Safety and environmental requirements - Part 2: design, construction, testing, marking and documentation*. Brussels: CENELEC; 2017. Standard No. SIST EN 378–2:2017.

[16] Nastic A, Jodoin B, Legoux JG, Poirier D. Particle impact characteristics influence on cold spray bonding: investigation of interfacial phenomena for soft particles on hard substrates. *J Therm Spray Technol*. 2021;30: 2013–33.

[17] Yin S, Suo X, Liao H, Guo Z, Wang X. Significant influence of carrier gas temperature during the cold spray process. *Surf Eng*. 2014;30(6): 443–50.

[18] Singh S, Raman RKS, Berndt CC, Singh H. Influence of cold spray parameters on bonding mechanisms: a review. *Metals*. 2021;11: 2016.

[19] Brusentseva T, Shikalov V, Lavruk S, Fomin V. Simulation of thermoplastic powder cold spraying. *J Sib Fed Univ Math Phys*. 2021;14(6): 726–34.

[20] Haban I, Sun Y, Veysset D, Nelson KA, Schuh CA. The effect of substrate temperature on the critical velocity in microparticle impact bonding. *Appl Phys Lett*. 2021;119: 011903

[21] da Silva FS, Bedoya J, Dosta S, Cinca N, Cano IG, Guilemany JM, et al. Corrosion characteristics of cold gas spray coatings of reinforced aluminum deposited onto carbon steel. *Corros Sci*. 2017;114: 57–71

[22] Winnicki M, Baszczuk A, Jasiorski M, Borak B, Małachowska A. Preliminary studies of TiO2 nanopowder deposition onto metallic substrate by low pressure cold spraying. *Surf Coat Technol*. 2019;371: 194–202

[23] Baszczuk A, Jasiorski M, Winnicki M. Low-temperature transformation of amorphous Sol–Gel TiO_2 powder to anatase during cold spray deposition. *J Therm Spray Tech*. 2018;27: 1551–62.

[24] Winnicki M. Advanced functional metal-ceramic and ceramic coatings deposited by low-pressure cold spraying: a review. *Coatings*. 2021;11: 1044.

[25] European Committee for Electrotechnical Standardization (CENELEC). *Aluminium and aluminium alloys - Chemical composition and form of wrought products - Part 3: chemical composition and form of products*. Brussels: CENELEC; 2014. Standard No. EN 573–3:2014.

[26] European Committee for Electrotechnical Standardization (CENELEC). *Welding consumables: wire electrodes, wires and rods for welding of aluminium and aluminium alloys: classification*. Brussels: CENELEC; 2016. Standard No. EN ISO 18273:2016.

[27] Massalski TB. *Binary alloys phase diagrams*. ASM International. Vol. 1; Ohio, 1992.

[28] Eustathopoulos N, Nicholas M, Drevet B. *Wettability at high temperatures. Pergamon materials series*. Pergamon, Oxford (UK). Vol. 3; 1999.

[29] Schwartz MM. Brazing, second edition. Mel M. Schwartz (Ed.) In: *The materials informations society*. Ohio (OH), USA: ASM International; 2003.

[30] Roberts P. *Industrial brazing practice*. 2nd ed. London: CRC Press. Taylor and Francis Group; 2013.

[31] Swiderski HW, Lauzon D. *Myths about aluminium brazing with non-corrosive fluxes NOCOLOK: Flux Brazing Technology. Materials of Solvay Flux GmbH*. May 2001, Aachen, Germany. Available from: `http://www.aluminium-brazing.com/sponsor/nocolok/Files/PDFs/31390.pdf`

[32] Swidersky HW, Ottmann A, Belt H. Comparison of flux characteristics and flux transfer systems in electrostatic NOCOLOK® flux application for aluminum brazing. Invitational aluminum brazing seminar: Thermal Alliance Internationl; Detroit, 1999.

[33] Milani SAAH. Effect of NOCOLOK flux dry-off temperature on mechanical properties of brazed joint for automotive aluminum-based heat exchangers. *Eng Res Ex-*

press. 2020;2: 025003.

[34] Wang Z, Cai S, Jin K, Wang X, Chen W. In-flight aggregation and deposition behaviour of particles in low pressure cold spray. *Surf Coat Technol*. 2021;409: 126875.

[35] Alonso L, Garrido MA, Poza P. An optimisation method for the cold-spray process: on the nozzle geometry. *Mater Des*. 2022;214: 110387.

[36] Buhl S, Breuninger P, Antonyuk S. Optimization of a laval nozzle for energy-efficient cold spraying of microparticles. *Mater Manuf Processes*. 2018;33(2): 115–22.

[37] Winnicki M, Piwowarczyk T, Małachowska A. General description of cold sprayed coatings formation and of their properties. *Bull Pol Acad Sci Techn Sci*. 2018;66(3): 301–10.

[38] Baranowski M, Bober M, Kudyba A, Sobczak N. The effect of surface condition on wetting of hastelloy® X by brazing filler metal of Ni-Pd-Cr-B-Si system. *J Mater Eng Perform*. 2019;28: 3950–9.

[39] Chung CL, Moon KS, Wong CP. Influence of flux on wetting behavior of lead-free solder balls during the infrared-reflow process. *J Electron Mater*. 2005;34: 994–1001.

[40] Yao Z, Xue S, Zhang J. Comparative study on the activity of GaF_3 and Ga_2O_3 nanoparticle-doped CsF-AlF_3 flux for brazing 6061 Al/Q235 steel joints. *Crystals*. 2020;10: 498–508.

[41] Nylén M, Gustavsson U, Hutchinson W, Karlsson Å, Johansson H. Mechanisms of erosion during brazing of aluminium alloys. *Mater Sci Forum*. 2002;396–402: 1585–90.

[42] Krystek K, Krzanowska K, Wierzbińska M, Motyka M. The effect of selected process conditions on microstructure evolution of the vacuum brazed joints of hastelloy X nickel superalloy sheet. *Arch Metall Mater*. 2022;67(4): 1551–61.

[43] Lacaze J, Tierce S, Lafont M-C, Thebault Y, Pébère N, Mankowski G, et al. Study of the microstructure resulting from brazed aluminium materials used in heat exchangers. *Mater Sci Eng A*. 2005; 413–414: 317–21.

Received 2023-01-10
Accepted 2023-03-08